



Gamma-ray polarization sensitivity of the Gammasphere segmented germanium detectors

G.J. Schmid*, A.O. Macchiavelli, S.J. Asztalos, R.M. Clark, M.A. Deleplanque, R.M. Diamond, P. Fallon, R. Kruecken, I.Y. Lee, R.W. MacLeod, F.S. Stephens, K. Vetter

Lawrence Berkeley National Laboratory, Nuclear Science Division, Building 88-111, 1 Cyclotron Road, Berkeley, CA 94720, USA

Received 27 June 1997; received in revised form 19 December 1997

Abstract

We present a technique for operating the Gammasphere segmented Ge detectors as γ -ray polarimeters. Using γ -rays of known polarization, we have measured the polarization sensitivity, $Q(E_\gamma)$, of these detectors in the energy range $E_\gamma = 0.4$ – 1.4 MeV. The experimentally obtained value of Q ranges from 5% at 415 keV to 4% at 1368 keV. The magnitude and energy dependence of $Q(E_\gamma)$ has also been determined theoretically by means of a Monte Carlo simulation, and the agreement between experiment and theory is within 20% over the energy range measured. In order to investigate the potential for operating Gammasphere as a γ -ray polarimeter in a high background environment (one which is typical of high-spin nuclear structure studies), we also discuss data that we have analyzed from the ^{176}Yb (^{26}Mg , 5n) ^{197}Pb reaction at $E = 135$ MeV. Although the polarimeter performance of Gammasphere is seen to be relatively poor, we are still able to demonstrate, by way of γ -ray polarization measurements, that “Shears Band 1” in ^{197}Pb should have negative parity. © 1998 Elsevier Science B.V. All rights reserved.

PACS: 24.70.+s; 29.30.kv; 29.40.-n

Keywords: Gamma-ray polarimeter; ^{197}Pb level scheme

1. Introduction

The Gammasphere array [1], currently located at the Argonne National Laboratory, is a 4π γ -ray detector used primarily for accelerator-based nu-

clear structure studies. In the “full-implementation” mode, gammasphere consists of 110 Compton suppressed, co-axial, germanium detectors. In order to reduce Doppler broadening effects in the γ -ray spectrum, approximately 70% of these detectors are segmented longitudinally. It has been suggested [2] that this segmentation could also be useful as a technique for measuring the γ -ray linear polarization.

In this paper, we document a series of experiments that have been done to quantify the γ -ray

*Corresponding author. Address for correspondence: Lawrence Livermore National Laboratory, Isotope Sciences Division, P.O. Box 808, L231, Livermore, CA 94551, USA. Tel.: (+1) 925-423-7866; e-mail: gjschmid@llnl.gov.

polarization sensitivity, $Q(E_\gamma)$, of the Gammasphere segmented Ge detectors. Data was acquired for the $^{24}\text{Mg}(p,p'\gamma)$ reaction at $E_p = 2.46$ MeV, the $^{56}\text{Fe}(p,p'\gamma)$ reaction at $E_p = 3.0$ MeV, and the $^{109}\text{Ag}(p,p'\gamma)$ reaction at $E_p = 2.54$ MeV. The reactions allow determination of $Q(E_\gamma)$ at the following energies (respectively): $E_\gamma = 1368$, 847 and 415 keV. The obtained results for $Q(E_\gamma)$ are compared with the performance of other recently built γ -ray polarimeters [3–5]. In addition to this experimental work, we discuss a full Monte Carlo simulation that has been done to determine, theoretically, the magnitude and energy dependence of $Q(E_\gamma)$ for the current segmented detectors. This allows reliable extrapolation of $Q(E_\gamma)$ to energies that were not explicitly measured.

In order to demonstrate how Gammasphere can be used as a Compton polarimeter, we also discuss here an analysis of $^{176}\text{Yb}(^{26}\text{Mg}, 5n)^{197}\text{Pb}$ data that was taken with Gammasphere in 1996 [6]. In this analysis, we concentrate on obtaining the sign of the γ -ray linear polarization, P , of the linking transition in ^{197}Pb between the bottom of “Band 1” and the known $I = 25/2^+$ spherical state [7]. We then use this sign to deduce the electric/magnetic (E/M) character of the transition. The results of this analysis can then be used to determine the parity of Shears Band 1. Based on a proposed configuration, a tentative assignment of negative parity has recently been made for this band [7]. The parity and configuration of Band 1 are of particular interest because its states are thought to arise from the “Shears” mechanism [8].

2. The Gammasphere segmented germanium detectors

2.1. Overview of design and operation

Fig. 1 shows the geometry of the Gammasphere coaxial segmented Ge detectors. The typical dimensions are as follows: diameter of 7 cm, length of 8 cm, and a co-axial hole diameter of 0.8 cm. A given Gammasphere detector will vary from these average dimensions by a few percent. The segmentation of the Ge detector is accomplished by means of a segmented outer contact rather than

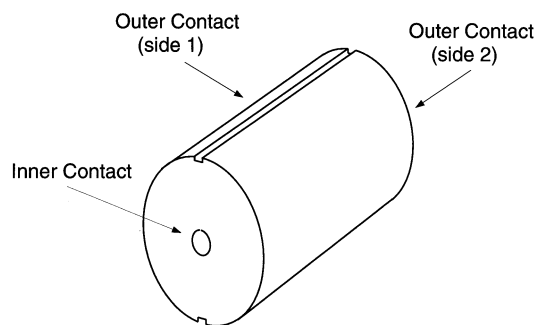


Fig. 1. The co-axial segmented Ge detectors which comprise $\sim 70\%$ of the Gammasphere array. The outer contact is segmented longitudinally to create two sides. When a γ -ray interacts in the crystal, the charge pulse height measured from one of these sides gives information about the energy deposited on that side of the crystal. The charge pulse height from the unsegmented inner contact gives information about the total energy deposited in the crystal.

a physical segmentation of the crystal. The signals which are read out by the associated electronics are a “full-energy” signal from the inner contact (which represents the total energy deposited on both sides of the detector), and a “side-energy” or “side-channel” signal from one of the segmented outer contacts (which represents the energy deposited on one side of the detector). The energy threshold on both the full-energy and side-energy signals is typically set at 60 keV.

Fig. 2 shows a comparison between the full-energy spectrum and the side-energy spectrum as acquired using a ^{152}Eu source. The larger background of the side-energy spectrum is due to the smaller volume of Ge covered by that signal. A very large difference in energy resolution between the full and side-energy spectra is also noticeable. The finite energy resolution of the full-energy spectrum ($\text{FWHM} = \Gamma = 2.5$ keV at 1.332 MeV) is due to the approximately equal contribution of two causes: statistics corresponding to the number of charge carriers released per γ -ray; and pre-amp noise. The energy resolution of the side-energy spectrum, on the other hand, is dominated by a capacitive noise component which arises because the side-channel signals are taken from the outer contact of the coaxial detector (which is close to the grounded Al can). Since this noise component is independent of γ -ray energy, the energy resolution of the side-energy

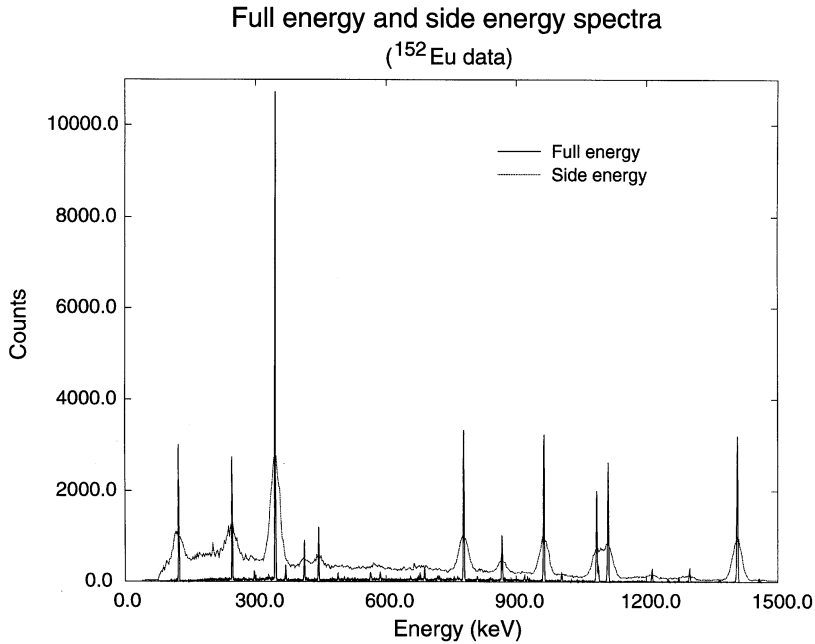


Fig. 2. The ^{152}Eu spectra measured using both the non-segmented inner contact (solid line) and one of the segmented outer contacts (dotted line).

spectrum is thus independent of energy, and has a typical value of about $\Gamma = 25$ keV. Fig. 3 shows the energy dependency of the energy resolution for both the full and side spectra.

2.2. Use for Doppler broadening correction

In typical heavy-ion reactions in nuclear structure studies, γ -rays can be emitted while the nucleus is in flight, and this leads to a third component to the energy resolution: the width due to Doppler broadening. With this third component, the general expression for the energy resolution can then be given as follows:

$$\Gamma_{\text{total}}^2 = \Gamma_{\text{statistics}}^2 + \Gamma_{\text{noise}}^2 + \Gamma_{\text{Doppler}}^2. \quad (1)$$

The Doppler shift of a γ -ray emitted by a nucleus in-flight is given by the following formula:

$$E = E_0 \left(1 + \frac{v}{c} \cos \theta \right), \quad (2)$$

where E_0 is the unshifted γ -ray energy, E is the Doppler shifted γ -ray energy, v is the velocity of the

recoiling nucleus in the lab frame (where we assume that $v \ll c$), and θ is the angle of the emitted γ -ray with respect to the beam direction.

Doppler broadening of spectrum peaks arise when the detector subtends a finite solid angle, and thus encounters a range of Doppler shifted energies from a given transition (since $E = E(\theta)$). The dependence of the broadening, $|\partial E|$, on θ is obtained by taking the partial derivative of Eq. (2)

$$|\partial E| = E_0 \frac{v}{c} \sin \theta \partial \theta, \quad (3)$$

where $\partial \theta$ can be taken to represent the opening angle of the detector as seen from the target.

Eq. (3) demonstrates that the Doppler broadening will be most significant at $\theta = 90^\circ$, and that in order to minimize the broadening, the opening angle of the detector must also be minimized. This line of reasoning motivated the segmentation of all Gammasphere Ge detectors in the neighborhood of 90° . The longitudinal segmentation shown in Fig. 1, when oriented in a direction perpendicular

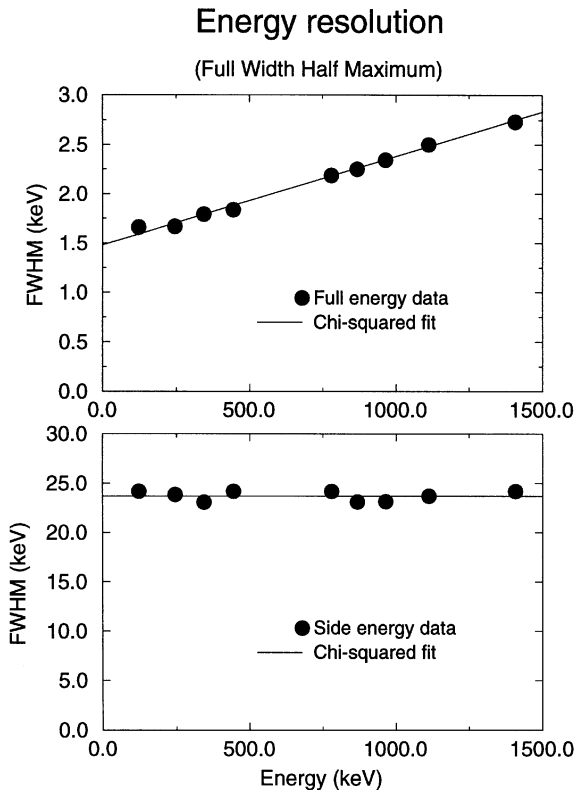


Fig. 3. The energy resolution of the full-energy channel (top) and side-energy channel (bottom) as determined from a ^{152}Eu source. The solid line represents a linear fit to the data (accomplished via χ^2 minimization).

to the beam direction, allows a reduction in the detector opening angle by essentially a factor of two, and this has allowed significant reductions of Doppler broadening, and thus significant improvements in overall detector resolution.

2.3. Use as a gamma-ray polarimeter

Although not designed with γ -ray polarization in mind, a Gammasphere segmented detector can be operated as a simple Compton polarimeter. In general, the principle behind a Compton polarimeter is to take advantage of the polarization dependence of the Compton scattering. This polarization dependence is expressed by the Klein–Nishina formula. After summing over outgoing polarization directions, the Klein–Nishina formula takes the

following form:

$$\frac{d\sigma}{d\Omega}(\theta_c, \phi_c) = \frac{1}{2} r_0^2 \frac{E'_\gamma{}^2}{E_\gamma^2} \left(\frac{E'_\gamma}{E_\gamma} + \frac{E_\gamma}{E'_\gamma} - 2 \sin^2 \theta_c \cos^2 \phi_c \right), \quad (4)$$

where $d\sigma/d\Omega$ is the differential cross section, r_0 is the classical electron radius, E_γ is the energy of the incident γ -ray, E'_γ is the energy of the Compton scattered γ -ray, θ_c is the polar Compton scattering angle, and ϕ_c is the azimuthal scattering angle (the angle between the electric vector of the incident γ -ray and the plane containing the incident and scattered γ -ray).

The Klein–Nishina formula (4) shows a clear preference for scattering into azimuthal directions which are perpendicular to the incident electric vector (i.e. $d\sigma/d\Omega$ is maximum for $\phi_c = 90^\circ$). By measuring an asymmetry between up–down (out-of-reaction-plane) and left–right (in-reaction-plane) scattering, one can seek to determine the polarization of a γ -ray beam. At low energies, Eq. (4) predicts that such an azimuthal asymmetry should be maximum for $\theta_c = 90^\circ$, and thus right-angle scattering is often employed. One standard polarimeter design consists of five elements lying in a plane perpendicular to the γ -ray beam direction: a central scatterer, and four “analyzing” detectors located at $\phi = 0^\circ$ (up), 90° (right), 180° (down), and 270° (left) with respect to the scatterer. Such a design was used in the “POLALI” polarimeter of [5]. This number of five total elements can easily be reduced to four because one of the analyzers can also serve as the scatterer. This yields the popular four-fold segmented design which has been the basis for several recent polarimeters ([3,4] and the “MINI-POLA” in Ref. [5]).

A two-fold segmented design, such as the one shown in Fig. 1, can also be used as a polarimeter by defining two experimental quantities of interest: the number of detector photopeak events which confine themselves completely to either one side or the other (the “confined” events); and the number of photopeak events that share the energy between the two sides (the “shared” events). Fig. 4 shows the situation whereby a γ -ray with its electric vector parallel to the line of segmentation is incident on the detector. Left–right scattering (most probable

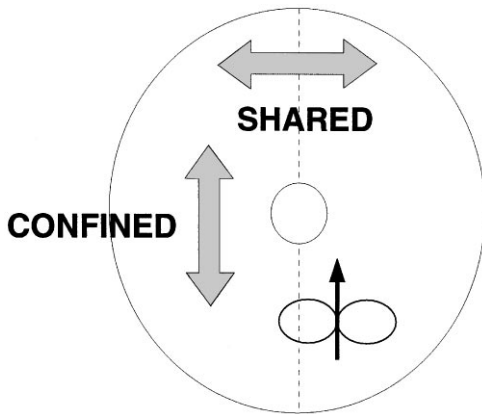


Fig. 4. The front face of a segmented Ge detector showing the co-axial hole and the effective line of segmentation. Incident γ -rays will scatter preferentially in a direction which is perpendicular to their electric vector. Events whereby the deposited energy is shared between the two sides is called “Shared”. Events which confine their energy entirely to one side or the other are called “Confined”.

in this case) will likely give a shared event. Up–down scattering with the geometry of Fig. 4 is more likely to give a confined event. The confined and shared events can then be used to calculate an experimental “asymmetry” which is analogous to the asymmetry of the four-fold segmented detector. This asymmetry can then be used to determine the γ -ray polarization. More details on this procedure appear in the next section.

3. Gamma-ray polarization formalism

3.1. Introduction

For a general review of the formalism of γ -ray polarization and γ -ray polarimeters, the reader is referred to the paper by Fagg and Hanna [9]. From Ref. [9], we get the standard definition of γ -ray linear polarization, $P(\theta)$, which is appropriate for nuclear reaction studies:

$$P(\theta) = \frac{J_0 - J_{90}}{J_0 + J_{90}}, \quad (5)$$

where J_0 is the average component intensity of the γ -ray electric vector in the reaction plane (the plane

containing the incident particle beam and the outgoing γ -ray), J_{90} is the intensity perpendicular to this plane, and θ is the angle of the polarimeter with respect to the incident beam direction.

Using the angular correlation formalism presented in Ref. [9], we can re-cast Eq. (5) into the following form:

$$P(\theta) = \frac{\sum_v a_v \kappa(LL') P_v^2(\cos \theta)}{1 + \sum_v a_v P_v(\cos \theta)}, \quad (6)$$

where the a_v coefficients are the normalized Legendre coefficients; the $P_v(\cos \theta)$ are the ordinary Legendre polynomials; the $P_v^2(\cos \theta)$ are the associated Legendre polynomials; and the $\kappa(LL')$ are quantities which depend on the multipolarities which are present (L, L'), and have their values given in Ref. [9]. Eq. (6) is required when one wants to extract $P(\theta)$ from an angular distribution measurement that has been fitted to Legendre polynomials.

3.2. Traditional formalism

Here we summarize the formalism that is associated with the recent four-fold segmented polarimeters of Refs. [3–5], and also with many of the polarimeters that have been developed during the past 30 yr (e.g. [10–13]). Section 3.3, which follows, contains the new definitions that are necessary to accommodate the different situation of the two-fold segmented detector.

When one measures an experimental asymmetry from a polarimeter, it is desirable that the result be directly proportional to $P(\theta)$. In particular, we want that

$$A(\theta) = Q(E_\gamma) P(\theta), \quad (7)$$

where the proportionality constant, $Q(E_\gamma)$, is the polarization sensitivity of the detector.

For a detector where up–down/left–right scattering asymmetries can be measured, the following formula for $A(\theta)$ is typically employed:

$$A(\theta) = \frac{N_V(\theta) - N_H(\theta)}{N_V(\theta) + N_H(\theta)}, \quad (8)$$

where N_V represents the number of vertical coincidences (i.e. up–down Compton scattering perpendicular to the reaction plane) and N_H the number of horizontal coincidences (i.e. left–right Compton scattering in the reaction plane).

If efficiency were not an issue, one could argue that the ideal polarimeter would consist of five point detectors: one central scatterer and four surrounding analyzers. If all these detectors were to lie in a plane perpendicular to the incident γ -ray direction, and if the azimuthal angle between the analyzers were 90° , it could then be shown, using Eqs. (4), (7) and (8) that

$$Q_p(E_\gamma) = \left(\frac{1}{E_\gamma/0.511 + 0.511/(E_\gamma + 0.511)} \right), \quad (9)$$

where $Q_p(E_\gamma)$ is the polarization sensitivity for point detector geometry. Finite geometry effects alter this energy dependence somewhat. However, it turns out that Eq. (9) often gives a fairly good approximation to the energy dependence of most Compton polarimeters (e.g. see discussion in Ref. [4]). In particular, it has become standard practice to normalize the form of Eq. (9) to the data by simply applying an overall multiplicative constant.

When one utilizes a polarimeter to make a γ -ray polarization measurement, the primary objective is to minimize the error in P . Using Eqs. (7) and (8), one can show that the error in P , ΔP , is related to Q as follows:

$$(\Delta P)^2 = \frac{1}{N_i Q^2 \varepsilon_c}, \quad (10)$$

where N_i is the total number of incident γ -rays and ε_c is the coincidence efficiency (i.e. the probability that an incident γ -ray registers a hit in both the scatterer and one of the analyzers). The form of Eq. (10) assumes that Q is very well known as compared with A (i.e. $\Delta Q \approx 0$). This condition can be realized by investing adequate time and effort in the calibration of the polarimeter.

For a given number of incident γ -rays, it has become standard to identify $Q^2 \varepsilon_c$, from Eq. (10), as a “figure of merit” (F) to be maximized. Thus, we have our final equation of interest:

$$F = Q^2 \varepsilon_c. \quad (11)$$

Based on a given counting time, F can be used to compare the relative performance of different polarimeters.

3.3. New definitions

For purpose of comparison with other standard polarimeters, we would like the Gammasphere segmented detectors to obey Eqs. (7) and (11). However, the two-fold segmented nature of the current geometry renders it impossible to measure a true up-down/left-right scattering asymmetry, and thus Eq. (8) cannot be used for $A(\theta)$. While a 90° rotation of the segmented Ge detectors about their axes would, in fact, allow such an up-down/left-right asymmetry to be measured, such rotations are not possible given the physical structure of the Gammasphere array.

In order to deduce a new form for $A(\theta)$ which is appropriate for non-rotatable bi-segmented Ge detectors, we introduce the following definitions:

$C_0, S_0 = \#$ of confined and shared events corresponding to an incident γ -ray beam in the pure J_0 state.

$C_{90}, S_{90} = \#$ of confined and shared events corresponding to an incident γ -ray beam in the pure J_{90} state.

$C_u, S_u = \#$ of confined and shared events corresponding to the case of unpolarized incident γ -radiation.

$C, S = \#$ of confined and shared events corresponding an incident γ -ray beam of arbitrary polarization. (12)

From these definitions, the following expressions are seen to be valid:

$$C_u = \frac{1}{2}(C_0 + C_{90}), \quad S_u = \frac{1}{2}(S_0 + S_{90}),$$

$$C_0 + S_0 = C_{90} + S_{90} = \varepsilon N, \quad (13)$$

where ε is the detector photopeak efficiency and N is the total number of γ -rays emitted from the source. The third expression is understood in the light of the cylindrical symmetry of the co-axial Ge detector. Independent of the orientation of the line of segmentation, the total number of counts detected, εN , should be constant.

For the case of arbitrary polarization, the following expressions are then seen to hold:

$$C = J_0 C_0 + J_{90} C_{90}, \quad S = J_0 S_0 + J_{90} S_{90}. \quad (14)$$

A natural guess for the form of $A(\theta)$ would be $(C - S)/(C + S)$. However, it can be shown using Eqs. (13) and (14) that this form is not factorable into the form of Eq. (7). Instead, we propose the following form for $A(\theta)$:

$$A(\theta) = \frac{1}{\sqrt{\eta}} \left(\frac{\eta C(\theta) - S(\theta)}{C(\theta) + S(\theta)} \right), \quad (15)$$

where $\eta = S_u/C_u$, and can (for example) be measured using an unpolarized radioactive source. Using Eqs. (13) and (14), we can show that Eq. (15) is factorable into the form which we desire

$$\begin{aligned} A(\theta) &= \frac{1}{\sqrt{\eta}} \left(\frac{C_0 - C_{90}}{C_0 + C_{90}} \right) \left(\frac{J_0(\theta) - J_{90}(\theta)}{J_0(\theta) + J_{90}(\theta)} \right) \\ &= Q(E_\gamma) P(\theta). \end{aligned} \quad (16)$$

Using Eqs. (7) and (15), we can derive the following formula for the error, ΔP , in the measured polarization, P :

$$\begin{aligned} (\Delta P)^2 &= \left(\frac{\Delta A}{Q} \right)^2 = \frac{1}{Q^2} \left[\left(\frac{\partial A}{\partial C} \right)^2 (\Delta C)^2 + \left(\frac{\partial A}{\partial S} \right)^2 (\Delta S)^2 \right] \\ &= \frac{1}{Q^2} \left[\frac{CS(\eta + 1)^2}{\eta(S + C)^3} \right]. \end{aligned} \quad (17)$$

Furthermore, if we assume that $\eta C \approx S$, and thus that $C + S \approx C(\eta + 1) = N_p = \varepsilon N_i$ (where N_p is the total number of detector photopeak events, ε is the photopeak efficiency, and N_i is the number of incident γ -rays), we can show that Eq. (17) yields the following form for the error in P :

$$\Delta P \approx \frac{1}{\sqrt{N_i}} \sqrt{\frac{1}{Q^2 \varepsilon}}, \quad (18)$$

where we again recover, in the denominator, the desired “figure of merit”, $F = Q^2 \varepsilon$ (except that this time, ε is the photopeak efficiency rather than the coincidence efficiency). This recovery of the standard form for F is due to the $1/\sqrt{\eta}$ factor which we have included in Eq. (15).

4. Measurements of $Q(E_\gamma)$

4.1. Overview

The procedure used in the measurement of $Q(E_\gamma)$ is similar to that of Ref. [4]. Using γ -rays of known polarization, asymmetries were measured in the Gammasphere segmented detectors and $Q(E_\gamma)$ was then determined using Eq. (7). In particular, data were acquired for the $^{24}\text{Mg}(p,p'\gamma)$ reaction at $E_p = 2.46$ MeV, the $^{56}\text{Fe}(p,p'\gamma)$ reaction at $E_p = 3.0$ MeV, and the $^{109}\text{Ag}(p,p'\gamma)$ reaction at $E_p = 2.54$ MeV. The targets used were natural magnesium, natural iron, and natural silver. At the time of this experiment, the Gammasphere array was located in Building 88 (Cave 4C) at the Lawrence Berkeley National Laboratory (LBNL), and thus the proton beams were provided by the LBNL 88” Cyclotron. For each reaction, the incident beam energy was chosen so as to strongly populate one of the first excited states in the target nucleus. The de-exciting γ -rays, at $E_\gamma = 1368$ keV in ^{24}Mg , 847 keV in ^{56}Fe , and 415 keV in ^{109}Ag , are all known to be pure $E2$ in nature. By measuring the angular distribution associated with each transition (by means of the Gammasphere array), the γ -ray polarizations can then be determined using Eq. (6). This information, combined with the asymmetries measured using the segmented detectors, allowed the determination of $Q(E_\gamma)$.

4.2. Angular distributions

The spectra acquired for the calibration reactions were exceptionally clean. The full-energy spectrum for $^{24}\text{Mg}(p,p'\gamma)$ is shown in Fig. 5. The acquired angular distributions for each of the reactions are shown in Fig. 6. The solid line is a Legendre polynomial fit to the data. Since the transitions are all known to be pure $E2$, we can then use the acquired a_2 and a_4 coefficients in Eq. (6) to get the expected $P(\theta)$ distribution. These $P(\theta)$ distributions are shown in Fig. 7. Because the polarization is strongest at 90° , the analysis with the segmented detectors has concentrated on this angle. Table 1 lists, for each reaction, the γ -ray energy, the a_2 and a_4 coefficients, and the predicted $P(90^\circ)$.

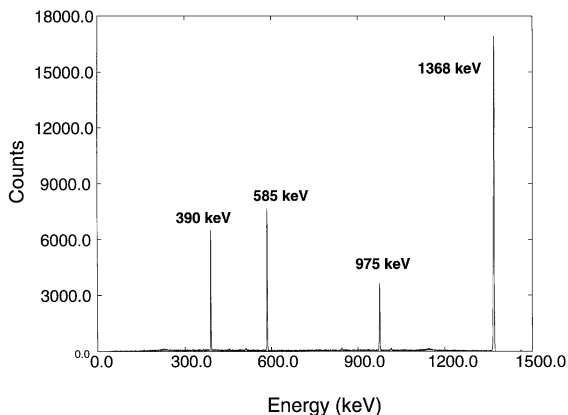


Fig. 5. The “full-energy” spectrum, as acquired from the inner contact, for the $^{24}\text{Mg}(p,p'\gamma)$ experiment. The 1368 keV line is the $2^+ \rightarrow 0^+$ transition of interest in ^{24}Mg . The other transitions shown are from the ^{25}Mg which is present in the natural Mg target.

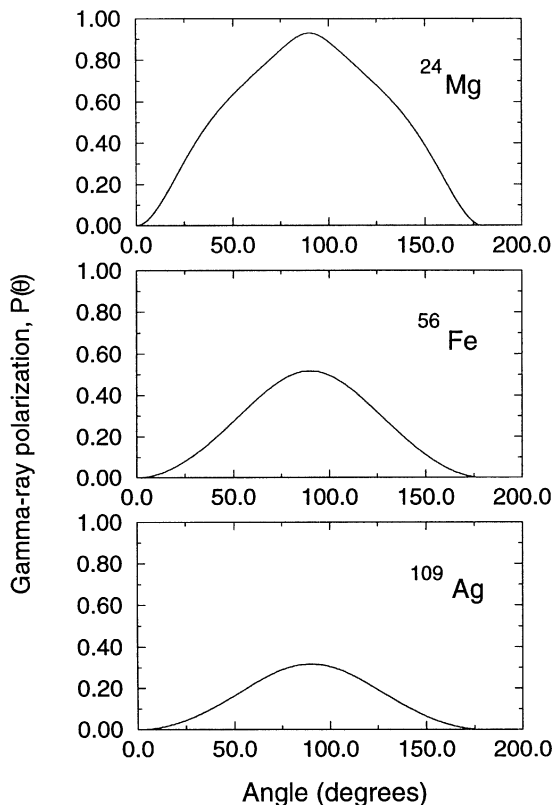


Fig. 7. The expected γ -ray polarizations as a function of angle for the three calibration reactions. These curves are calculated from the angular distributions in Fig. 6, taking into account the known $E2$ character of the transitions.

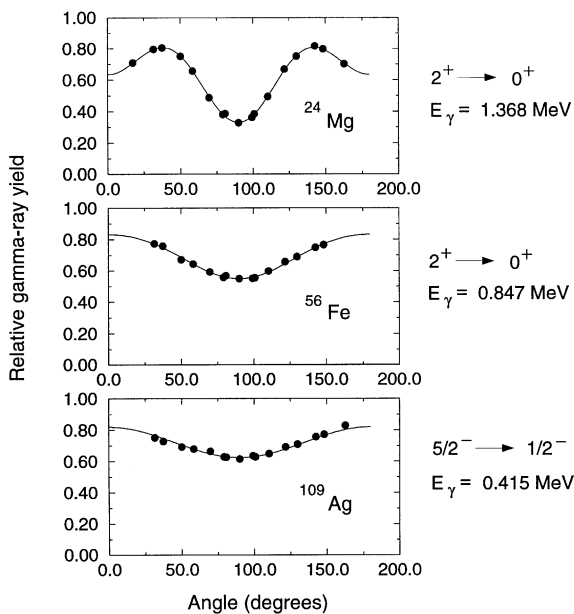


Fig. 6. Angular distributions for the $(p,p'\gamma)$ reactions studied. In each case, the γ -ray of interest is the transition from one of the first excited states to the ground state of the target nucleus.

4.3. Segmented detector asymmetries

For each experiment, side-energy spectra were acquired for both the in-beam reaction of interest

(e.g. $^{24}\text{Mg}(p,p'\gamma)$) and also for a ^{152}Eu source, which serves as a source of unpolarized γ -rays from 100 to 1400 keV. To calculate $A(90^\circ)$ from Eq. (15), we need the confined (C) and shared (S) events from the in-beam experiment as well as the ^{152}Eu data for calculating the $\eta(E_\gamma)$ values. Since the energies afforded by the ^{152}Eu source do not (in general) correspond exactly to the desired γ -ray energy of the in-beam experiment, a procedure is needed for obtaining a suitable value of η . If the desired energy lies close to a ^{152}Eu line, simple linear interpolation is valid. Otherwise, a theoretical energy dependence is needed (see Section 5).

In the current series of calibration measurements, side-energy spectra at 90° (i.e. spectra derived from one of the outer contacts of a segmented

Table 1
Experimental results leading to determination of the polarization sensitivity, Q , for the segmented Ge detectors

Target	E_p (MeV)	E_γ (MeV)	a_2	a_4	$P(90^\circ)$	$A(90^\circ)$	Q
^{24}Mg	2.46	1.368	0.540 ± 0.002	-0.473 ± 0.002	0.931 ± 0.007	0.040 ± 0.002	0.043 ± 0.002
^{56}Fe	3.0	0.847	0.302 ± 0.003	-0.031 ± 0.003	0.520 ± 0.006	0.025 ± 0.003	0.047 ± 0.005
^{109}Ag	2.54	0.415	0.191 ± 0.003	0	0.317 ± 0.005	0.017 ± 0.002	0.052 ± 0.007

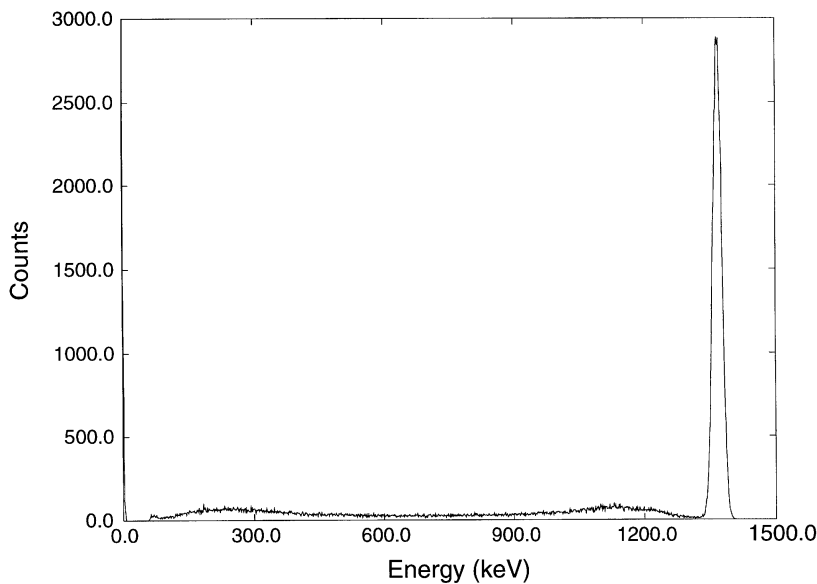


Fig. 8. A side-energy spectrum for $^{24}\text{Mg}(p,p'\gamma)$ which has been gated on the 1368 keV line in the full-energy spectrum. The strong peak in this spectrum at 1368 keV represents events confined to one side, while the zeros (events that the ADC has sorted into channel zero because there is no coincidence present) represent events confined to the other side.

detector at $\theta = 90^\circ$) were acquired in a coincidence mode by gating on the peak of interest in the full-energy spectra (the spectra derived from the inner contact). As an example, the gated side-energy spectrum for $^{24}\text{Mg}(p,p'\gamma)$ is shown in Fig. 8. The shape of this spectrum represents the distribution of deposited energy (for the 1368 keV line) within the crystal. An event is classified as confined (C) or shared (S) using the following criteria: all events located within 2 FWHM of the peak are

considered confined to one side; all events from this point down to just above the zero channel are considered shared; and all events in the zero channel (which represent events where the full energy signal is above the 60 keV threshold, but the side energy signal is not) are considered confined to the other side. The two confined totals are then summed together to produce one overall confined figure.

Having acquired confined and shared events for each transition of interest, we can then use Eq. (15)

to determine $A(90^\circ)$ and Eq. (7) to determine $Q(E_\gamma)$ (making use of the $P(90^\circ)$ values from the angular distribution measurements). The results are shown in Table 1.

4.4. Comparison of results to other polarimeters

Using the traditional “figure of merit”, $F = Q^2\varepsilon$, we can obtain a rough comparison between the current two-fold segmented design and previous four-fold segmented designs (where $\varepsilon = \varepsilon_c$). For the 1368 keV line, Table 2 shows the comparison of Q , ε , and F for the polarimeter of Schlitt et al. [3], the POLALI polarimeter of Ref. [5], the MINIPOLA of Ref. [5], and the current polarimeter. This “figure of merit” comparison would indicate that the current design is competitive with those of Refs. [3,5] (the results in Ref. [4] do not include an absolute determination of F). In particular, it is seen that the gain in ε over ε_c more than compensates for the lower Q of the current polarimeter. In an array with many detectors, such as Gamma-sphere, the “figure of merit” takes on the form: $F = N_d Q^2\varepsilon$, where N_d is the number of detectors involved in the measurement. With 77 segmented detectors, Gamma-sphere can potentially be very powerful in this respect.

In practice, however, comparisons using F are not always valid. It often turns out to be more important to obtain a clean spectrum than to obtain a spectrum with a lot of counts (e.g. if the count rate is very high, the counting time is no longer a limiting factor). In this case, Q (which is directly proportional to the measured asymmetry) is the

important quantity. In this regard, the current polarimeter, with its relatively low Q , is not seen to be competitive with other recent polarimeters.

5. Monte Carlo simulation

5.1. Overview

In order to extrapolate $Q(E_\gamma)$ to energy regions where data was not acquired, experimenters typically fit their data to a theoretical energy dependence. For standard four-fold segmented detectors, it has been empirically found that $Q_p(E_\gamma)$, the polarization sensitivity for “point-detector” geometry, is often an adequate energy dependence. However, the current data, due to the different two-fold geometry, is not well fit by this form. With this motivation, a theoretical effort was pursued to calculate $Q(E_\gamma)$ for the current geometry by means of a Monte Carlo simulation. Since commercially available codes could not be found which incorporated γ -ray polarization effects, a completely new program was written. The basic idea of this new code was to model the source–detector geometry in an exact fashion, and then simulate the multiple Compton scattering of the incident γ -rays inside the Ge crystal (for the geometry in question, each 1 MeV γ -ray Compton scatters ~ 5 times before photoabsorption). Although similar in many ways to standard Monte Carlo treatments, the novel aspect of this code was the rigorous handling of the γ -ray polarization effects in the multiple scattering. This was accomplished by taking the analytical

Table 2
Polarimeter comparison

Polarimeter	Q at 1.368 MeV	Efficiency at 1.368 MeV	Figure of merit (F)
3	0.15	4.4×10^{-5} (Coincidence efficiency)	1.0×10^{-6}
5 (POLALI)	0.30	2.0×10^{-5} (Coincidence efficiency)	1.8×10^{-6}
5 (MINIPOLA)	0.05	1.2×10^{-5} (Coincidence efficiency)	3.0×10^{-8}
Gamma-sphere segmented Ge detector	0.04	9.0×10^{-4}	1.7×10^{-6}

approach derived by Wightman [14] and applying it to the Monte Carlo method. Full details of this program are discussed elsewhere [15], but we present some of the results below.

5.2. Results of simulation for unpolarized observables

In order to test the validity of the Monte Carlo simulation discussed above, a calculation of the segmented Ge detector efficiency (for the full-energy signal) was undertaken. The calculation involved a single detector at 25 cm from a 1.332 MeV γ -ray source (on-axis). The result predicted that the photopeak efficiency should be 78% as compared with a $3'' \times 3''$ NaI(Tl) detector at the same distance. The statistical error in this calculation was better than 1%. An experimental determination of the photopeak efficiency, obtained by taking an average of the measurements for many detectors, gave 74%. This is within 5% of the calculated value.

Another unpolarized quantity that is of interest is $\eta(E_\gamma)$. If a $Q(E_\gamma)$ measurement is required where no $\eta(E_\gamma)$ data exist, a theoretical prediction for $\eta(E_\gamma)$ can be used. Fig. 9 shows the $\eta(E_\gamma)$ data acquired using a side-energy threshold of 130 keV. These data are derived from the strong lines measured

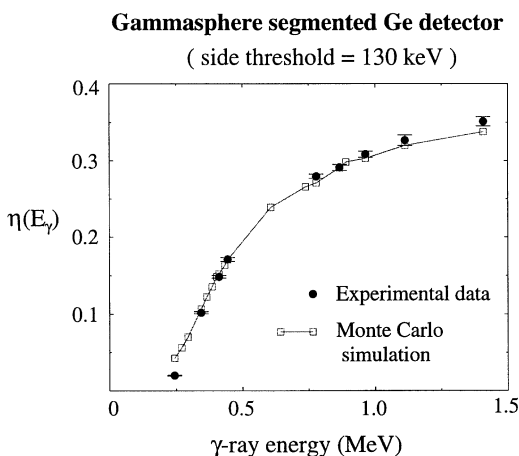


Fig. 9. A graph of the $\eta(E_\gamma)$ parameter, showing both experiment (solid points) and theory (open points connected by straight lines).

using a ^{152}Eu source. For comparison, Monte Carlo simulations for $\eta(E_\gamma)$ were done at each γ -ray energy in ^{152}Eu (a few extra energies were also added). These calculations were not normalized to the data in any way. The agreement between the data and the Monte Carlo simulation is excellent.

5.3. Results of simulation for $Q(E_\gamma)$

Fig. 10 shows the result of the Monte Carlo simulation for $Q(E_\gamma)$ as compared with the measured data. The agreement is within 20% over the energy region measured. The “turn over” of the curve at lower energies is especially noticeable. This facet of the energy dependence is to be expected due to the decreased mean free path for the γ rays at the lower energies. In particular, if the γ -rays cannot reach the other side of the detector by one, or several, scatterings, virtually all events will be confined, and $Q(E_\gamma)$ will be very low.

In order to understand the 20% discrepancy between theory and experiment, Monte Carlo simulations were undertaken whereby the inner and outer radius of the Ge detector were varied. To a good approximation, the effect was to scale $Q(E_\gamma)$

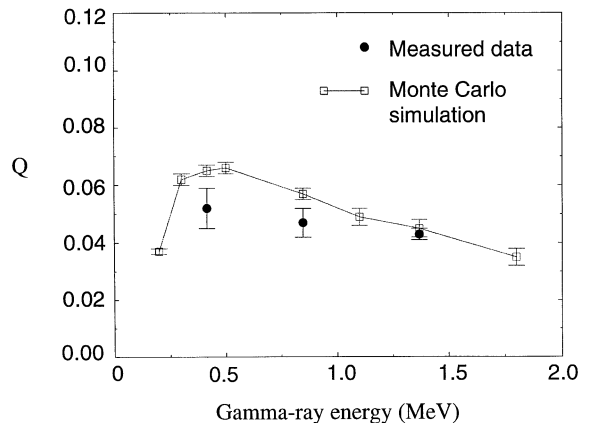


Fig. 10. A graph of the polarization sensitivity, $Q(E_\gamma)$, showing both experiment (solid points) and theory (open points connected by straight lines). In calculating Q , the energy threshold for the shared events was set at 60 keV (i.e. if the side energy was less than 60 keV for a fully absorbed γ -ray, the event was classified as a confined event).

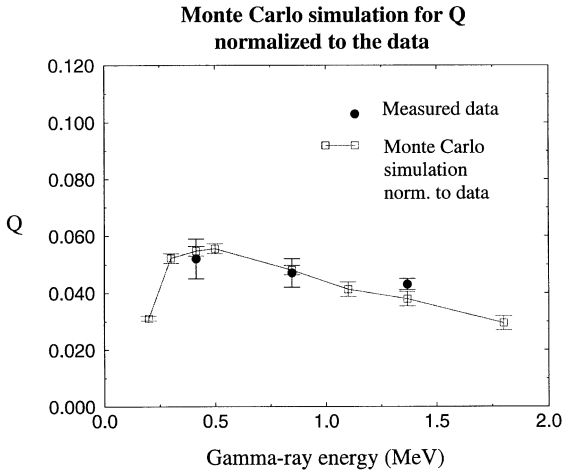


Fig. 11. The $Q(E_\gamma)$ curve normalized to the experimental data by means of an overall multiplicative constant.

up or down by a constant multiplicative factor. Therefore, if we make the assumption that the discrepancy between theory and data is due to uncertainties in the Ge detector geometry (e.g. crystal dimensions, dead layers, etc.), we can make a first-order correction by simply multiplying the theoretical curve by a constant so as to normalize it to the data. We can accomplish this by minimizing a χ^2 function. The resulting curve is shown in Fig. 11. Using this curve, we can now obtain a reasonable estimate for Q at all energies.

6. Gamma-ray polarization measurement in ^{197}Pb

6.1. The experiment

To illustrate the technique that we have developed for γ -ray polarization measurements, we discuss here some γ -ray data that we have analyzed from the $^{176}\text{Yb}(^{26}\text{Mg},5n)^{197}\text{Pb}$ reaction at $E = 135$ MeV. The experiment was performed at the LBNL 88" Cyclotron. The ^{176}Yb target was thick enough to completely stop the ^{197}Pb recoils, and thus (due to the relatively long lifetimes of the γ -ray transitions) Doppler broadening in the γ -ray spectrum was not an issue. The segmented Ge detectors that we looked at were the 12 detectors located between 80 and 100° (with respect to the beam

axis). These detectors were gain matched (both full-energy and side-energy channels), and had their side-energy thresholds all set at 60 keV. During data acquisition, the confined and shared events for each detector were summed to produce a single confined and shared value for each γ -ray transition of interest.

The specific goal of this analysis was to experimentally determine the parity of Band-1 in ^{197}Pb . This band is thought to arise from the ‘‘Shears’’ mechanism [7], a new concept in nuclear structure physics. Fig. 12 shows the most recent level scheme proposed for this nucleus [7]. A determination of $E1$ character for the 432 keV linking transition at the bottom of the band would confirm the tentatively assigned negative parity shown in Fig. 12. Since photons of electric character should have their electric vectors in the reaction plane (as defined by the beam axis and the γ -ray direction), and since the line of segmentation of the Ge detectors is always perpendicular to the reaction plane, we expect to measure a positive asymmetry (A), and therefore a positive polarization, for an $E1$ transition. On the other hand, the in-band transitions of band-1 are thought to be primarily $M1$ in character due to the nature of the Shears mechanism. For these transitions we would expect to measure a negative asymmetry, and therefore a negative polarization.

6.2. Expected magnitude of polarization for the in-band and linking transitions

Using tables of angular distribution functions for maximum possible alignment (e.g. Ref. [16]), along with Eq. (6), one can show that the maximum polarization for pure dipole transitions at high (half-integer) spin is 36%. Using $A = PQ$ at 400 keV (where $Q \sim 5\%$), we see that we must look for experimental asymmetries which are at most 2%, and perhaps as low as 1% (when one accounts for the effects of incomplete alignment).

Recasting the form of Eq. (15), we obtain

$$A(\theta) = \frac{1}{\sqrt{\eta}} \left(\frac{\eta C(\theta)/S(\theta) - 1}{C(\theta)/S(\theta) + 1} \right). \quad (19)$$

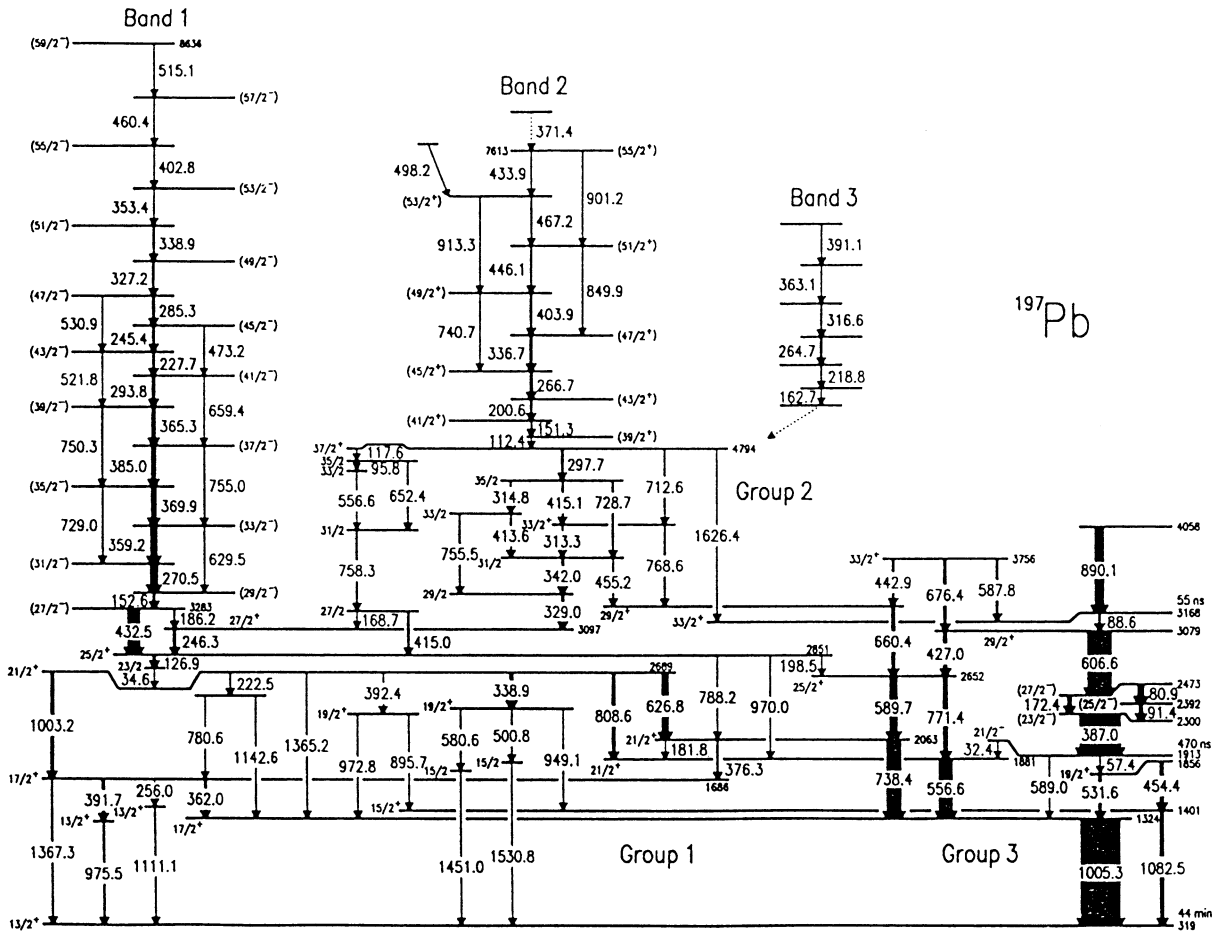


Fig. 12. The most recent level scheme for ^{197}Pb as presented in Ref. [7].

From Eq. (19), we see that it is not the absolute confined and shared peak areas that we are after, but rather the confined-to-shared yield ratio. In this manner, we can hope that systematic effects in the peak fitting procedure will cancel out to some extent.

6.3. Polarization results

Fig. 13 shows an acquired spectrum for Band-1 after gating on the 270 keV in-band transition. The gated spectra (both confined and shared) were then analyzed to obtain the peak areas, and thus the experimental asymmetries and measured polarizations, for the following transitions: 353, 294, 365,

385, 370, 359 keV (all in-band), and also the 432 keV linking transition. The peak areas were obtained by way of a peak fitting program (DAMM from Oak Ridge National Laboratory) which allowed simultaneous fitting of multiple peaks and background. The number of peaks included per fit was kept to a minimum consistent with the requirement that a good χ^2 per degree of freedom be obtained (for a small fitting region, a constant peak width vs. energy was assumed). The measured asymmetries are listed in Table 3 and the resulting polarizations are graphed in Fig. 14. The error bars in the table and the figure are derived from parameter errors in the peak fitting procedure.

In Fig. 14, the 432 keV linking transition appears strongly positive, consistent with an assumption of $E1$ character. In contrast, the in-band transitions appear negative, consistent with the assumption of $M1$ character. These results support the assumption of negative parity for Band-1 in ^{197}Pb , and are in agreement with the polarization results of Eurogam [17]. The fact that some of the transitions

show unrealistically high polarization magnitudes ($> 36\%$), and the fact that the in-band transitions show significant scatter about an average value, suggests that accurate polarization measurements using Gammasphere may not be possible in high spin experiments which involve (heavy ion, xn) reactions. This would be due to the associated high

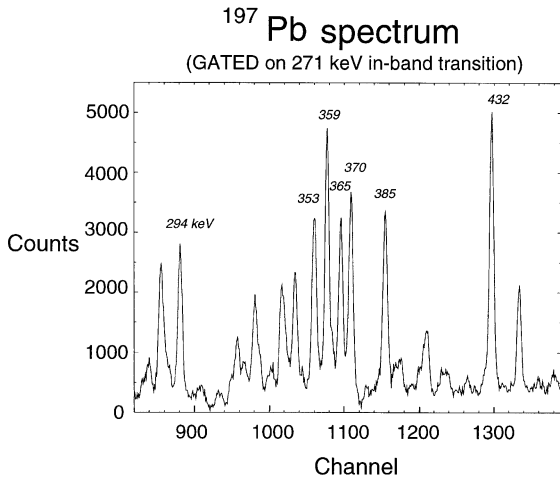


Fig. 13. Confined spectrum from the $^{176}\text{Yb}(^{26}\text{Mg},5n)^{197}\text{Pb}$ reaction at $E = 135$ MeV. This spectrum is generated from the 12 segmented Ge detectors between 80 and 100° . The spectrum is gated on the 270 keV in-band transition.

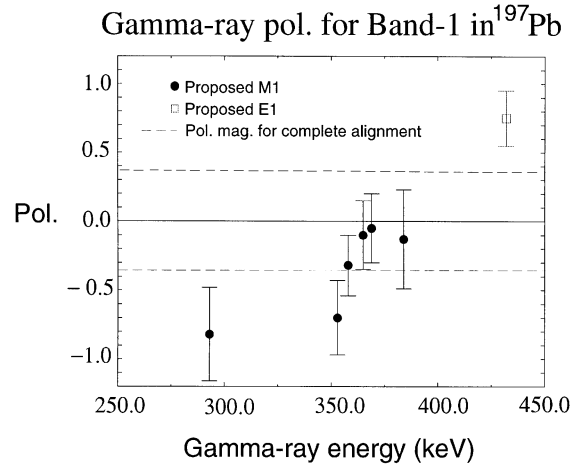


Fig. 14. Results for the γ -ray polarization, P , of the in-band transitions (solid points) and the 432 keV linking transition (open point). Error bars are derived from the errors in peak fitting parameters. The dashed lines show the magnitude of polarization which would be expected for maximum alignment.

Table 3

Calculation of gamma ray polarizations for transitions in ^{197}Pb (measurements made at $\theta_{\text{lab}} = 90^\circ$)

	353 keV Transition	294 keV Transition	365 keV Transition	384 keV Transition	369 keV Transition	358 keV Transition	432 keV Transition
Proposed multipolarity	$M1$	$M1$	$M1$	$M1$	$M1$	$M1$	$E1$
η from ^{152}Eu	0.105 ± 0.002	0.061 ± 0.001	0.116 ± 0.002	0.130 ± 0.002	0.120 ± 0.002	0.112 ± 0.002	0.163 ± 0.003
Confined (C)	20583 ± 412	16622 ± 266	19691 ± 394	20601 ± 618	23513 ± 470	28817 ± 576	30934 ± 402
Shared (S)	2450 ± 98	1226 ± 82	2320 ± 93	2747 ± 137	2840 ± 114	3425 ± 103	4449 ± 125
Asymmetry, $A(90^\circ)$	-0.039 ± 0.015	-0.045 ± 0.019	-0.005 ± 0.014	-0.007 ± 0.020	-0.003 ± 0.014	-0.018 ± 0.012	0.041 ± 0.011
Polarization, $P(90^\circ)$	-0.70 ± 0.27	-0.82 ± 0.34	-0.10 ± 0.25	-0.13 ± 0.36	-0.05 ± 0.25	-0.32 ± 0.22	0.75 ± 0.20

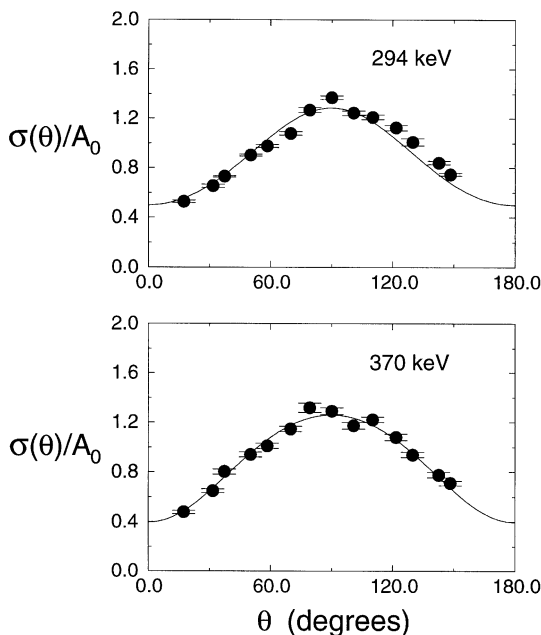


Fig. 15. Angular distributions for the two in-band transitions in ^{197}Pb which differ most in their polarization magnitude (Fig. 14). The solid line is a Legendre fit which includes the a_2 and a_4 coefficients.

ambient background which limits the accuracy to which one can fit peak areas.

To verify that the scatter in the in-band polarizations is due to peak fitting problems, and not an actual variance of the $E2/M1$ in-band ratio (which could also give polarization changes), we investigated the angular distribution for each transition. Fig. 15 shows the angular distributions that correspond to the two in-band transitions which varied most in polarization magnitude: the 294 keV line and the 370 keV line. The solid lines in Fig. 15 are the results of a Legendre polynomial fit using the a_2 and a_4 coefficients. The deviation of the points from the smooth lines (in particular, the perceived asymmetry in the 294 keV case) are indicative of unknown systematic error, probably due to the peak fitting procedure. However, the curves are quite similar, and the extracted a_2 and a_4 coefficients differ only slightly outside of error. Using the formalism of Ref. [16], we can relate the measured a_2 and a_4 coefficients to the $E2/M1$ mixing ratio associated with maximum possible alignment. In

this manner, we find a constant mixing ratio of $\sim 10\%$ for all the transitions. This seems to back up the assertion that the apparent changes in polarization values are due to peak fitting problems, and not a physical effect (e.g. some effect related to the Shears mechanism).

Since the γ -ray background for high-spin studies is typically quite high, and since the currently studied band is strong in comparison with other high spin bands (e.g. the other Shears bands in the Pb isotopes), it is not clear to what extent Gammasphere can be useful as a general polarimeter in the high spin regime. Acquiring adequate statistics for double or triple gating would be one possible technique for further cleaning up the spectra, and thus improving the performance of Gammasphere polarimetry. Another possible step to improve performance would be to alter the Gammasphere support structure so as to allow rotation of each segmented Ge detector about its axis. This would make it possible to measure an up-down/left-right scattering asymmetry with a given detector (via a 90° rotation), and would thus eliminate the need for the $\eta(E_\gamma)$ parameter. This would help reduce possible sources of systematic error.

7. Conclusion

Although Gammasphere was not originally designed to function as a γ -ray polarimeter, we have investigated here its potential to operate as such. In particular, we have measured the γ -ray polarization sensitivity, $Q(E_\gamma)$, for the Gammasphere segmented Ge detectors over a range of energies. We have then applied this knowledge to a direct measurement of γ -ray polarizations in ^{197}Pb .

The spread of the in-band polarization data shown in Fig. 14 indicates that the segmented Ge detectors are not able to operate as sensitive polarimeters in a high background environment. This problem is directly related to the low polarization sensitivity (Q) of the current two-fold segmented geometry. However, it would appear that with a careful measurement, one can still hope to differentiate between electric and magnetic transitions in the spectrum. The current γ -ray polarization study that we have done in ^{197}Pb

demonstrates a different sign in γ -ray polarization between the proposed $M1$ transitions and the proposed $E1$ transition. This evidence supports the contention [7,17] that Shears Band-1 in ^{197}Pb has negative parity.

Acknowledgements

The authors thank the staff of the 88" Cyclotron at Berkeley for their support. In addition, the authors would like to thank Dr. Dave Ward for helpful discussions. This work was supported by the US Dept. of Energy under contract #DE-AC03-76SF00098.

References

- [1] I.Y. Lee, Nucl. Phys. A 520 (1990) 641c.
 [2] A.O. Macchiavelli et al., Conf. on Phys. from Large Gamma-ray Det. arrays, Proc., vol. 2, Lawrence Berkeley Laboratory, 1994, p. 149.
 [3] B. Schlitt, U. Maier, H. Friedrichs, S. Albers et al., Nucl. Instr. and Meth. A 337 (1994) 416.
 [4] P.M. Jones, L. Wei, F.A. Beck, P.A. Butler et al., Nucl. Instr. and Meth. A 362 (1995) 556.
 [5] A. von der Werth, F. Becker, J. Eberth et al., Nucl. Instr. and Meth. A 357 (1995) 458.
 [6] R.M. Clark et al., to be published.
 [7] G. Baldsiefen, S. Chmel, H. Hubel et al., Nucl. Phys. A 587 (1995) 562.
 [8] G. Baldsiefen, H. Hubel, W. Korten et al., Nucl. Phys. A 547 (1994) 521.
 [9] L.W. Fagg, S.S. Hanna, Rev. Mod. Phys. 31 (1959) 711.
 [10] A.E. Litherland, G.T. Ewan, S.T. Lam, Can. J. Phys. 48 (1970) 2320.
 [11] P.A. Butler, P.E. Carr, L.L. Gadeken, A.N. James et al., Nucl. Instr. and Meth. 108 (1973) 497.
 [12] R. Bass, S. Brinkmann, C. vonCharzewski, H. Hanle, Nucl. Instr. and Meth. 104 (1972) 33.
 [13] J. Simpson, P.A. Butler, L.P. Ekstrom, Nucl. Instr. and Meth. 204 (1983) 463.
 [14] A. Wightman, Phys. Rev. 74 (1948) 1813.
 [15] G.J. Schmid et al., to be published.
 [16] E. Der Mateosian, A.W. Sunyar, Atomic data and Nucl. data tables 13 (5) (392) 1974.
 [17] H. Hubel, Private Communication.